

# **Structural Condition Assessment of Asphalt Pavement Semi-Rigid Bases Using FWD Deflection Basin Parameters**

Linyi Yao<sup>b</sup>, Jiwang Jiang<sup>a,\*</sup>, Changbo Li<sup>c</sup>, Zhen Leng<sup>b</sup>, Fujian Ni<sup>a</sup>

<sup>a</sup> Department of Highway and Railway Engineering, School of Transportation, Southeast University, Nanjing, Jiangsu, China

<sup>b</sup> Department of Civil and Environmental Engineering, The Hong Kong Polytechnic University, Hung Hom, Kowloon, Hong Kong

<sup>c</sup> China Railway 19th Bureau Group No. 3 Engineering Co., Ltd., Shenyang 110136, China

\* Corresponding author

Email: [jiang\\_jiwang@seu.edu.cn](mailto:jiang_jiwang@seu.edu.cn)

# Structural Condition Assessment of Asphalt Pavement Semi-Rigid Bases Using FWD Deflection Basin Parameters

Assessing structural conditions of semi-rigid bases in asphalt pavements is essential for effective base treatment in reconstruction and expansion (R&E) projects. Although various falling weight deflectometer (FWD) parameters have been developed for this purpose, field-validated parameters are still missing. This study identifies the appropriate FWD deflection basin parameter (DBP) through sensitivity analysis, correlation examination, and on-site milling and inspection. Findings indicate D20-D60 as the most suitable DBP, with 23  $\mu\text{m}$  and 40  $\mu\text{m}$  thresholds for warning and severe conditions, respectively. The correlation between D20-D60 and cracking rate suggests that high cracking rates suggest base weakness, whereas low rates may not guarantee structural integrity due to maintenance masking effects. On-site milling further confirmed this finding, demonstrating the alignment between D20-D60 assessments and field observations. The outcome of this study is anticipated to provide a practical DBP for evaluating semi-rigid base conditions and to inform base treatment strategies in R&E projects.

*Keywords:* Falling weight deflectometer, Deflection basin parameter, Semi-rigid base, Asphalt pavement, Structural condition.

## 1 Introduction

Since the first expressway in China was constructed in 1988, expressway construction has made rapid progress over the past two decades. By the end of 2023, the expressway mileage in China reached 184,000 kilometers. A large portion of these expressways have exceeded the 15-year design life required by the current design specifications of China (Ministry of Transport of the People's Republic of China, 2017). Taking Jiangsu province as an example, about 64% of the expressways have served for more than 15 years. Long-term service has led to the gradual deterioration of road infrastructure and the emergence of various functional and structural distresses (Yao et al., 2022; Liang et al., 2023). On the other hand, traffic demand is also increasing. Both of these have led to a growing demand for road reconstruction and expansion (R&E) to improve the overall performance of pavements, accommodate the ever-increasing traffic volume, and ensure a sustainable and efficient transportation network (Xu et al., 2024; Ye et al., 2019). To reduce R&E costs and conserve resources, it is crucial to retain and reuse as much of the existing pavement materials and structures as possible. One of the

key concerns in this process is whether the existing pavement structure is still functional and performing as required (Li et al., 2023; Xiong et al., 2023), particularly the underlying base layers that have received minimal maintenance. Addressing this concern necessitates rigorous testing and assessment of the structural condition of the base course, which is essential not only for determining treatment strategies for existing base course but also for ensuring the longevity and functionality of the newly reconstructed roads.

In China, over 90% of expressway pavements utilize semi-rigid bases constructed from cement or lime-fly-ash stabilized materials (Dong et al., 2021), owing to their high stiffness and cost-effectiveness. Typical methods for assessing the structural condition of semi-rigid bases include core drilling and testing, Benkelman beam method, falling weight deflectometer (FWD) deflection testing, and ground-penetrating radar (GPR) (Zang et al., 2018; Deng and Yang, 2019; Jing et al., 2020; Liu et al., 2023; Cheng et al., 2024). Among these methods, FWD is a non-destructive testing device widely used globally. It is designed to simulate the load of a wheel passing over the pavement and measure the resulting deflection basin, which varies depending on the stiffness and thickness of each pavement layer (Elshaer et al., 2020). Based on the FWD deflection basin, the back-calculation of pavement structure modulus can be achieved (Pożarycki et al., 2019; Kutay et al., 2011). However, the back-calculated modulus sometimes fails to characterize the actual pavement structural condition due to its susceptibility to initial values, unstable convergence, and poor accuracy, particularly in areas with cracks (Cui et al., 2018; Ma et al., 2019).

The strong correlation between the geometric characteristics of the deflection basin and the structural strength of the pavement has prompted many studies to propose various deflection basin parameters (DBPs) and utilize them to evaluate the pavement structural condition. The widely used DBPs can be divided into three categories: radius of curvature (RoC) parameters, area parameters, and slope parameters. RoC refers to the radius of a circle centered at a point above the load center, with its circumference passing through two points on the deflection basin (Dehlen, 1962; Horak and Emery, 2009). The principle is that as the RoC decreases, the deflection basin becomes deeper, indicating weaker pavement strength. Area parameters quantify the normalized area of a vertical slice through a deflection basin, measured from the center of the test load to various radial distances from it (Hoffman, 1980). They are typically used to evaluate the structural condition of the entire pavement structure (de Andrade et al., 2023). Slope parameters measure the relative change between two points on the deflection basin, i.e., the deflection difference between the measuring points. The most widely used slope parameters include the surface curvature index (SCI), base damage index (BDI), and base curvature index (BCI) (Talvik and Aavik, 2009; Donovan and Tutumluer, 2009; Vaitkus et al., 2021; Vyas et al., 2021; Fuentes et al., 2022), which have been proven to be effective indicators for assessing the structural condition of the surface layer, base layer, and subgrade, respectively (de Andrade et al., 2023; Jiang et al., 2022). In addition to these parameters, other DBPs used in the literature and practice include shape factor, deflection ratio, and single-point deflection values (Ma et al., 2019; Talvik and Aavik, 2009; Pierce et al., 2017).

For the base layer, BDI, defined as the difference between the deflections measured at 30 cm and 60 cm from the center of the loading plate, is the most widely used parameter for characterizing its structural condition (de Andrade et al., 2023; Kim, 1998; Park et al., 2005; Nguyen et al., 2023). The suitability of this parameter is usually verified by evaluating the sensitivity of the theoretical BDI values to the base modulus (Jiang et al., 2022; Xu et al., 2002; Rabbi and Mishra, 2021), investigating the correlation between the field BDI values and base stiffness indicators (Park et al., 2005), checking whether the BDI can distinguish between intact and damaged base layers (Kim, 1998) or between base layers with different materials (de Andrade et al., 2023), and visual distress surveys (Rabbi and Mishra, 2021). However, previous highway FWD deflection surveys revealed

an inflection point in the deflection basin at 20 cm from the loading point (Cui et al., 2018). Specifically, the deflection basin exhibits a concave shape between 0 and 20 cm, transitioning to a convex shape beyond 20 cm. Therefore, further examination and validation are needed to determine whether  $D_{20}$ - $D_{60}$  ( $D_x$  denotes the deflection value measured by the sensor at  $x$  cm from the loading point) is more suitable than  $D_{30}$ - $D_{60}$  for assessing the structural condition of semi-rigid bases. Moreover, while various verification methods exist, the most direct and convincing approach is to visually confirm whether the structural conditions indicated by the parameters align with the actual conditions in the field. The problem is that visual distress surveys do not necessarily reflect the structural condition of the underlying pavement layers. Therefore, this study aims to determine the appropriate parameter for assessing the structural condition of semi-rigid base layers and to validate the parameter through on-site milling in a real-world R&E project.

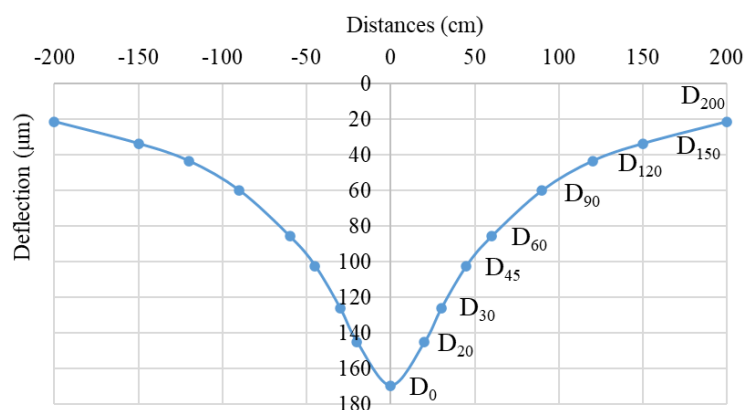
## 2 FWD Data Collection and Processing

### 2.1 FWD measurement

FWD tests simulate the effect of a moving wheel load by dropping a known weight from a specified height onto a circular loading plate placed on the pavement surface to generate an impulse load (Ministry of Transport of the People's Republic of China, 2019). This action generates a deflection bowl, a measurable deformation pattern that reflects the pavement's response to the load, as shown in Figure 1. The deflections are recorded by sensors placed at various distances from the load plate, providing detailed data on the pavement's stiffness and structural condition. A sensor should be placed at the center of the loading plate, with additional sensors arranged linearly from the center, typically distributed within 250 cm. For back-calculating the modulus of the pavement structure layer, a minimum of seven sensors (preferably nine) are required, including positions at 0 cm, 30 cm, 60 cm, and 90 cm (Ministry of Transport of the People's Republic of China, 2019). Each measurement point is tested at least three times. The first drop is considered a preparatory drop and discarded due to the unstable contact between the loading plate, deflection sensors, and the pavement (Ministry of Transport of the People's Republic of China, 2019). The load and deflection data from the second and subsequent drops are recorded to ensure statistically meaningful averages.



(a) FWD



(b) Deflection basin curve

Figure 1 Schematic diagram of FWD deflection testing

### 2.2 Temperature corrections

The need for temperature correction in deflection measurements arises from the temperature sensitivity of asphalt mixtures. As the temperature increases, the modulus of the surface asphalt mixture decreases, resulting

in a change in the shape of the deflection basin. Therefore, the correction of deflection values is closely related to the modulus of the surface layer and can be achieved by correcting the surface layer modulus. Specifically, the surface layer modulus was varied while keeping the moduli of the base, subbase, and subgrade constant to derive the theoretical deflection basin through the multi-layer linear elastic method (Rabbi and Mishra, 2021). The correlation between the main deflection differences and the surface layer modulus was then established as shown in the following equation:

$$\lg(\Delta D) = a \lg(E_1) + b \quad (1)$$

where  $\Delta D$  represents the main deflection differences ( $D_0-D_{20}$ ,  $D_0-D_{30}$ ,  $D_0-D_{45}$ ,  $D_0-D_{60}$ ,  $D_0-D_{90}$ ,  $D_0-D_{120}$ ,  $D_0-D_{150}$ ,  $D_0-D_{180}$ , and  $D_0-D_{210}$ ),  $E_1$  is the modulus of the surface layer, and  $a, b$  are the regression coefficients. According to equation (1), the following relationship can be derived.

$$K = \frac{\Delta D_s}{\Delta D} = \left(\frac{E_{1s}}{E_1}\right)^a \quad (2)$$

where  $K$  is the temperature correction factor,  $\Delta D_s$  is the deflection difference at standard temperature (20°C), and  $E_{1s}$  is the modulus of the surface layer at standard temperature (20°C).

The U.S. Federal Highway Administration (FHWA) has developed a formula for adjusting the back-calculated asphalt modulus according to temperature (FHWA, 2000), as shown follows:

$$ATAF = 10^{\text{slope}(T_r - T_m)} \quad (3)$$

where  $ATAF$  is the asphalt temperature adjustment factor,  $T_r$  is the reference temperature (°C),  $T_m$  is the measured temperature (°C), and  $\text{slope}$  is the slope of the equation for the logarithm of the asphalt modulus and temperature, and is recommended to be -0.0195 for the measurement point at the wheel track and -0.021 for the measurement point in the middle of the lane. Based on equations (2) and (3), the temperature correction factor,  $K$ , can be derived as follows:

$$K = ATAF^a = 10^{\text{slope}(T_r - T_m)a} \quad (4)$$

Other temperature-corrected deflection differences can also be calculated, such as  $D_{20}-D_{60}$  at standard temperature:

$$(D_{20} - D_{60})_s = (D_0 - D_{60})K_{D_0-D_{60}} - (D_0 - D_{20})K_{D_0-D_{20}} \quad (5)$$

### 3 DBPs for Base Structure Conditions

#### 3.1 Proposal of DBPs

Among the three main types of DBPs, the area parameter is usually used to evaluate the condition of the entire pavement structure, whereas RoC is reported to have poor correlation with base materials other than flexible structures (de Andrade et al., 2023). Therefore, the traditional parameter for evaluating the condition of the base structure, BDI, is a slope parameter. Meanwhile, previous studies have shown that the stress diffusion from the FWD loading point to the pavement structure generally follows the “2-3” rule (Zhang et al., 2003), that is, most deflections measured on the pavement surface originate from below a line angled 34 degrees from the horizontal, as illustrated in Figure 2. Based on this principle, the deflection difference measured on the pavement surface between an offset of 1.5 times the thickness of the asphalt surface layer and an offset of 1.5 times the total thickness of the surface and the base layer originates entirely from the base layer. Taking the

expressways in Jiangsu Province as an example, the total thickness of the three-layer asphalt surface ranges from 12 to 24 cm, averaging around 18 cm. The total thickness of the surface and base layer ranges from 32 to 61 cm, averaging around 56 cm. Therefore, the deflection differences measured by sensors between 20 cm and 90 cm may constitute suitable parameters for assessing the structural condition of the base layer of typical pavement structures in China. Based on this consideration, four candidate DBPs were evaluated, including  $D_{20}$ - $D_{60}$ ,  $D_{30}$ - $D_{60}$ ,  $D_{30}$ - $D_{90}$ , and  $(D_{30}-D_{60})/D_{30}$ .

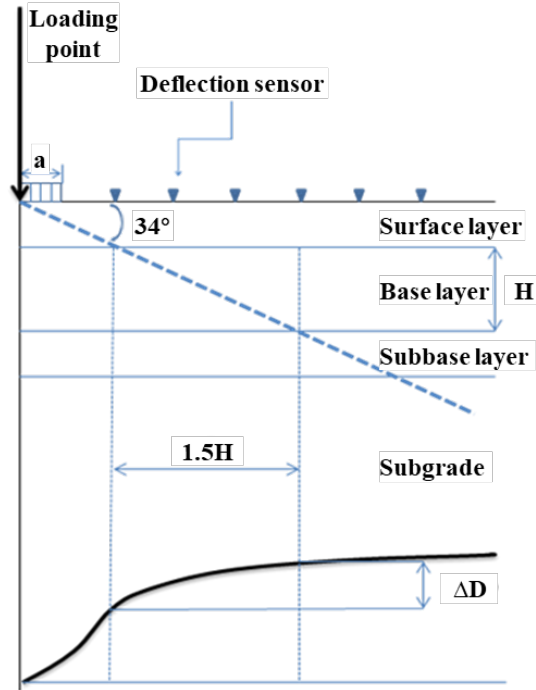


Figure 2 Schematic diagram of stress diffusion angle

### 3.2 Parameter evaluation

The initial evaluation and verification of DBPs would be conducted from two perspectives: examining the sensitivity of theoretical DBP values to the base modulus and analyzing the correlation between measured DBP values and the back-calculated base modulus. These processes will utilize deflection basin data from the Jiangsu section of the Beijing-Shanghai Expressway, as this dataset is more comprehensive and larger in volume. A subsequent case study for field validation will focus on a real-world R&E project on a major expressway in Northeast China. The actual condition of the base structure will be visually inspected after milling the pavement structure layer by layer to verify the consistency between assessment results and observed conditions. Additionally, the application of DBPs derived from Jiangsu's expressways to assess the structural conditions of expressways in Northeast China further highlights the parameter's applicability and generalizability.

#### 3.2.1 Theoretical deflection basin

Taking the Beijing-Shanghai Expressway, Jiangsu Section as an example, the base modulus was varied from 3000 MPa to 25000 MPa. Theoretical deflection basins were then obtained using the multi-layer linear elastic method, and the values of the candidate DBPs were calculated. Figure 3 presents the relationship between the DBPs and the base layer modules, where the secondary vertical axis (deflection difference-deflection ratio) refers to DBPs like  $(D_{30}-D_{60})/D_{30}$ . The observation reveals that the four candidate DBPs, which characterize the structural condition of the base layer, decrease as the base modulus increases, displaying a power function

relationship. Among them, parameters  $D_{20}$ - $D_{60}$  and  $D_{30}$ - $D_{60}$  exhibit the most significant variations and are therefore the most sensitive to changes in base modulus.

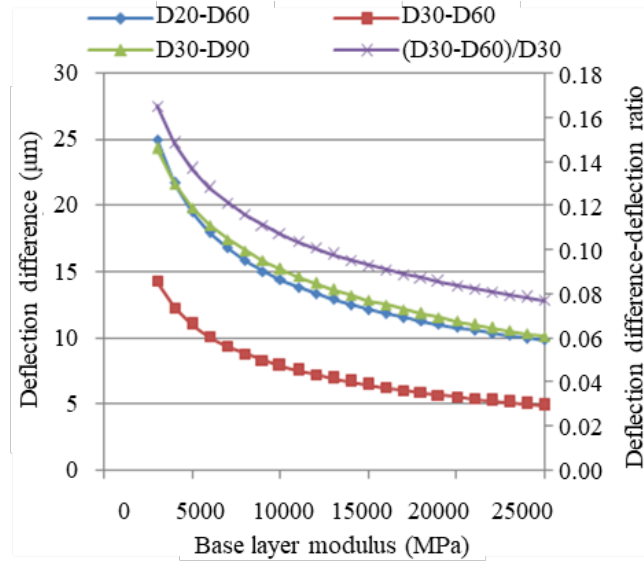
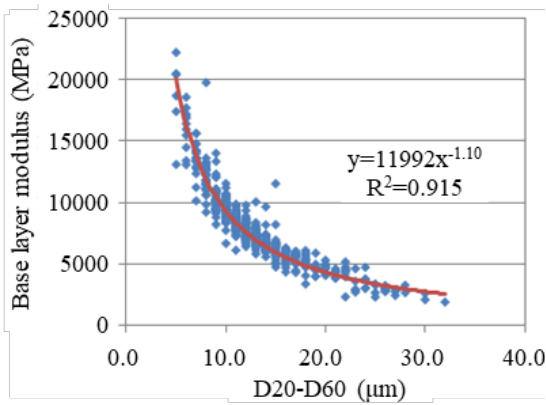


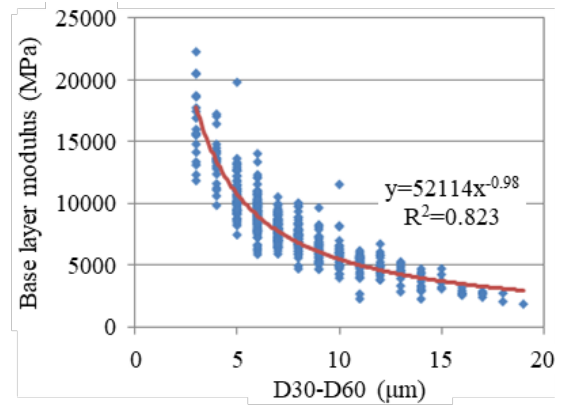
Figure 3 Relationship between theoretical DBPs and base layer modules

### 3.2.2 Measured deflection basin

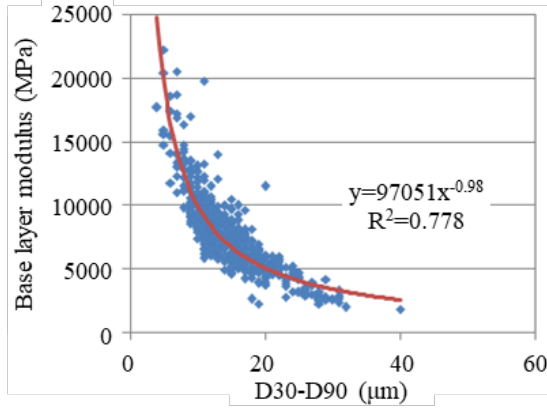
The base modulus was back-calculated using field FWD deflection basin data collected on the Beijing-Shanghai Expressway, Jiangsu Section. Several well-known modulus back-calculation software programs, such as EVERCALC, MODULUS 6.0, and MICHBACK, were compared. Ultimately, the software that demonstrated better applicability for semi-rigid base asphalt pavements with relatively thin asphalt layers and high base modulus, along with more consistent and stable back-calculation results, was selected for base modulus back-calculation. A regression analysis was performed to explore the correlation between the back-calculated base modulus and each DBP, as illustrated in Figure 4. It can be observed that the back-calculated base modulus correlates best with  $D_{20}$ - $D_{60}$ . Combining with the results of theoretical deflection basin analysis,  $D_{20}$ - $D_{60}$  was determined to be the appropriate DBP characterizing base structure conditions.



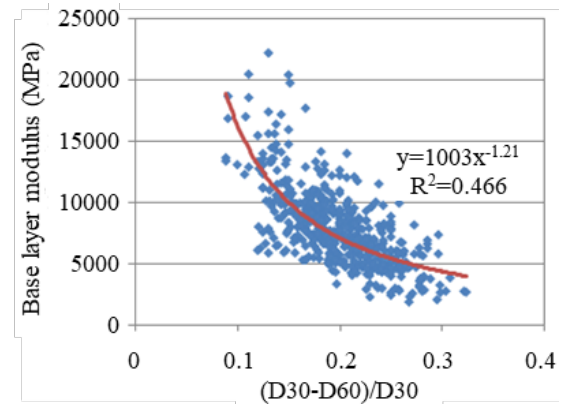
(a)  $D_{20}$ - $D_{60}$



(b)  $D_{30}$ - $D_{60}$



(c)  $D_{30}-D_{90}$



(d)  $(D_{30}-D_{90})/D_{30}$

Figure 4 Relationship between measured DBPs and back-calculated base layer modulus

### 3.3 Parameter threshold

Furthermore,  $D_{20}-D_{60}$  data from sections with and without base maintenance history on the Beijing-Shanghai Expressway, Jiangsu Section were compared, as shown in Figure 5. For sections with base maintenance history, the  $D_{20}-D_{60}$  data were collected from the last FWD deflection test conducted before maintenance implementation. The distance discrimination method was used to determine the boundary value between the two datasets, and the data on both sides of the boundary were discriminated as belonging to different categories (with or without base maintenance history). Consequently, this study identified 23  $\mu\text{m}$  as the boundary value, marking the threshold at which the condition of the semi-rigid base structure reaches the warning levels and may require maintenance. Additionally, the  $D_{20}-D_{60}$  values for sections without a history of base maintenance were all below 40  $\mu\text{m}$ . Therefore, 40  $\mu\text{m}$  can be used as the threshold for  $D_{20}-D_{60}$  to indicate a severe condition that necessitates base maintenance.

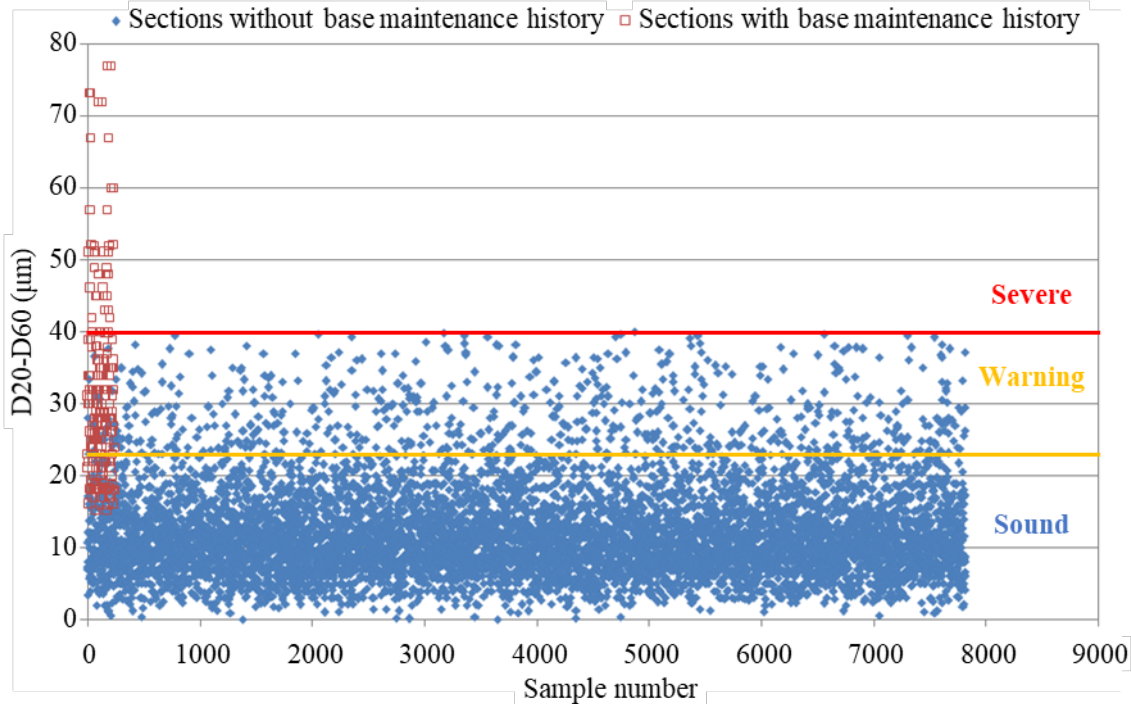


Figure 5 Scatterplot of  $D_{20}-D_{60}$  for sections with and without base maintenance history



## 4 Case study

The proposed DBP was utilized to assess the structural condition of the existing base layer in a real R&E project. Validation of this parameter was conducted in the field by milling the pavement structure layer by layer and visually inspecting the structural integrity of the base layer.

### 4.1 Case information

The R&E project is located on a major highway in northeastern China, which has been in operation for over 20 years. The original roadway, designed as a six-lane dual carriageway, is now inadequate due to increasing traffic volumes and the deterioration of pavement performance. As a result, an expansion to a ten-lane dual carriageway is required to meet current demands. The original pavement structure comprises a 16cm asphalt surface layer, a 40 cm semi-rigid base layer, and a 17cm cushion layer, as listed in Table 1.

Table 1 Original pavement structure information

Layer	Definition
Upper layer	4cm AK-13 (with SBS modified asphalt)
Middle layer	5cm AC-20 (with SBS modified asphalt)
Lower layer	7cm AC-30 (with base binder asphalt)
Base layer	40cm cement-stabilized macadam
Cushion layer	17cm graded gravel

Notes: AK=an anti-skid asphalt mixture gradation; SBS=styrene-butadiene-styrene; AC=asphalt concrete;

The long-term service of the highway leads to severe pavement aging and various distresses, including cracking, rutting, potholes, and raveling. Historical maintenance treatments primarily involved milling and resurfacing the asphalt surface layer to restore functional performance rather than enhance overall structural strength. Notably, the base layer has never been maintained during its 20-year service life. Historical FWD testing data indicate that the average deflection from 2007 to 2020 increased by approximately 33%, signifying a corresponding reduction in the pavement structure's overall strength. Therefore, a comprehensive investigation into the structural condition of the existing base layer is essential to guide treatment strategies for the base layer during the R&E project.

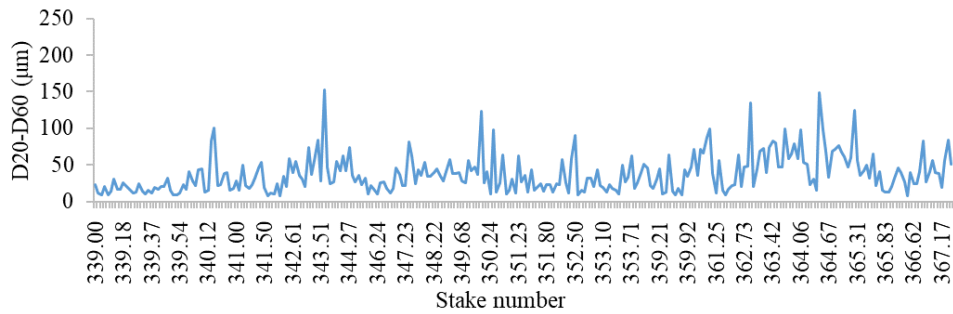
Prior to the FWD test, a field survey was conducted to evaluate pavement conditions. This involved using an automated pavement inspection vehicle to measure rutting depth and performing manual visual inspections to identify cracks. The FWD test collected deflection basin data for each lane (excluding bridge decks) in one direction, covering a section of nearly 30km. Data was collected at approximately 50-meter intervals, with a total of 274 sets from the passing lane, 291 sets from the middle lane, 279 sets from the driving lane, and 37 sets from the right hard shoulder. Additionally, detailed investigations were conducted at 5-meter intervals in selected typical sections.

### 4.2 Results and discussion

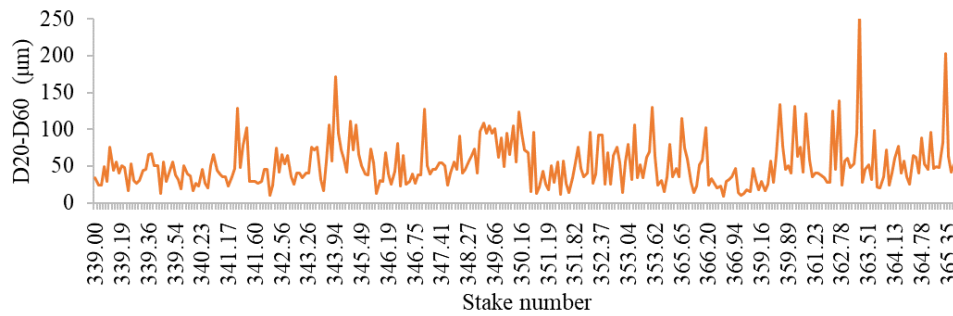
#### 4.2.1 Distribution of $D_{20}$ - $D_{60}$

Figure 6 shows the distribution of the  $D_{20}$ - $D_{60}$  parameter along the stake number for the three lanes. Table 2 presents the descriptive statistics of  $D_{20}$ - $D_{60}$  for different lanes. The maximum value of the  $D_{20}$ - $D_{60}$  parameter is 257  $\mu\text{m}$ , while the minimum value is only 3.8  $\mu\text{m}$ . The standard deviation is approximately 30  $\mu\text{m}$ , and the coefficient of variation is around 65%. Figure 6 and Table 2 indicate a high dispersion of the  $D_{20}$ - $D_{60}$  data, reflecting the parameter's sensitivity to base layer strength and the uneven distribution of base layer strength

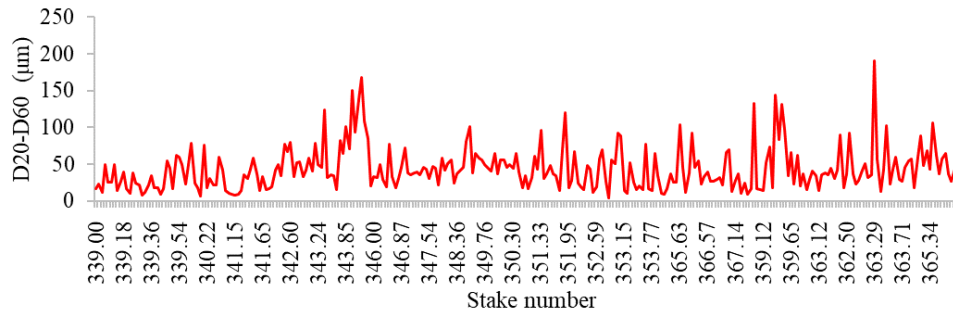
1 along the tested section. Comparing the different lanes, it can be observed that the mean  $D_{20}-D_{60}$  of the middle  
2 lane is the highest, suggesting that the overall condition of the base layer in the middle lane is worse than that  
3 of the other two lanes.



(a) Passing lane



(b) Middle lane



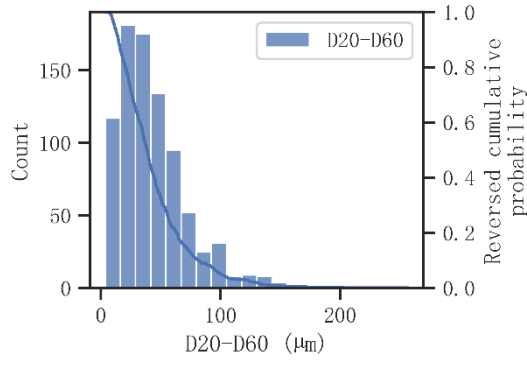
(c) Driving lane

Figure 6 Distribution of  $D_{20}-D_{60}$  along the stake number in different lanes

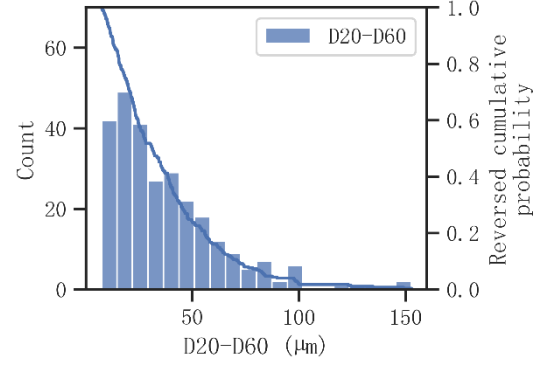
Table 2 Descriptive statistics of  $D_{20}-D_{60}$  in different lanes

Lane	Number of points	Mean ( $\mu\text{m}$ )	Standard deviation ( $\mu\text{m}$ )	Minimum ( $\mu\text{m}$ )	Maximum ( $\mu\text{m}$ )	Coefficient of variation
Passing lane	274	37.43	25.63	7.50	152.70	68.49%
Middle lane	291	52.22	31.85	9.40	257.00	61.00%
Driving lane	279	43.66	29.36	3.80	190.20	67.26%

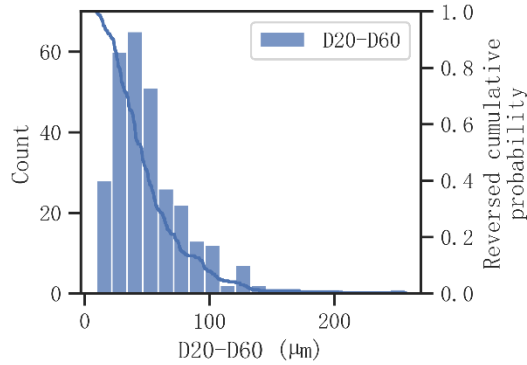
6 Figure 7 shows the probability distributions and reversed cumulative probability distributions of  $D_{20}-D_{60}$   
7 for different lanes as well as for the entire section. The reversed cumulative probability describes the cumulative  
8 probability of being greater than a specific  $D_{20}-D_{60}$  value. It was found that about 36.1%, 59.8%, and 45.2% of  
9 the  $D_{20}-D_{60}$  values exceeded the severe threshold of 40  $\mu\text{m}$ , indicating a high risk of insufficient base strength  
10 in the tested section.



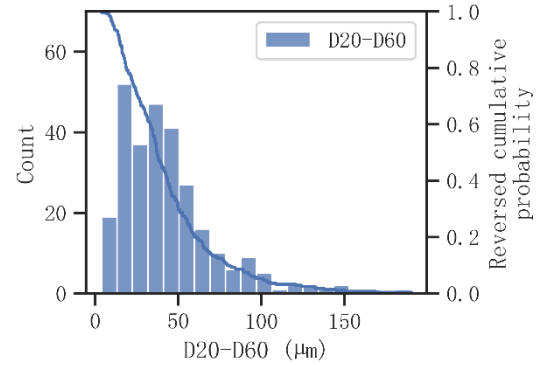
(a) Entire section



(b) Passing lane



(c) Middle lane



(d) Driving lane

Figure 7 Probability distributions of  $D_{20}-D_{60}$  in different lanes

#### 4.2.2 Correlation with pavement surface distresses

In the current research, only longitudinal, transverse, and alligator cracking were examined. These types of defects occur when the entire pavement or individual layers lack sufficient structural strength. A cracking rate index was used to integrate these types of cracks as shown in equation (6), where longitudinal and transverse cracks were converted to damaged area using an impact width of 0.2 m according to the specification (Ministry of Transport of the People's Republic of China, 2018).

$$Cracking\ rate = \frac{0.2 \cdot LLC + 0.2 \cdot LTC + AAC}{W \cdot L} \quad (6)$$

where  $LLC$  and  $LTC$  are the length of longitudinal and transverse cracks, respectively,  $AAC$  is the area of alligator cracks,  $W$  is the lane width, and  $L$  is the length of the section (1000m).

Figure 8 presents the correlation between  $D_{20}-D_{60}$  and the cracking rate. There is a positive linear relationship when the cracking rate exceeds 30%, but no significant relationship when the cracking rate is below 30%. A survey of pavement maintenance histories revealed that many sections with a cracking rate below 30% had undergone maintenance. Therefore, it can be concluded that while a high cracking rate can indicate insufficient base strength, low cracking rate does not necessarily imply an intact base structure, as pavement maintenance can restore surface conditions. This also demonstrates the importance of condition assessment of in-service base structures.

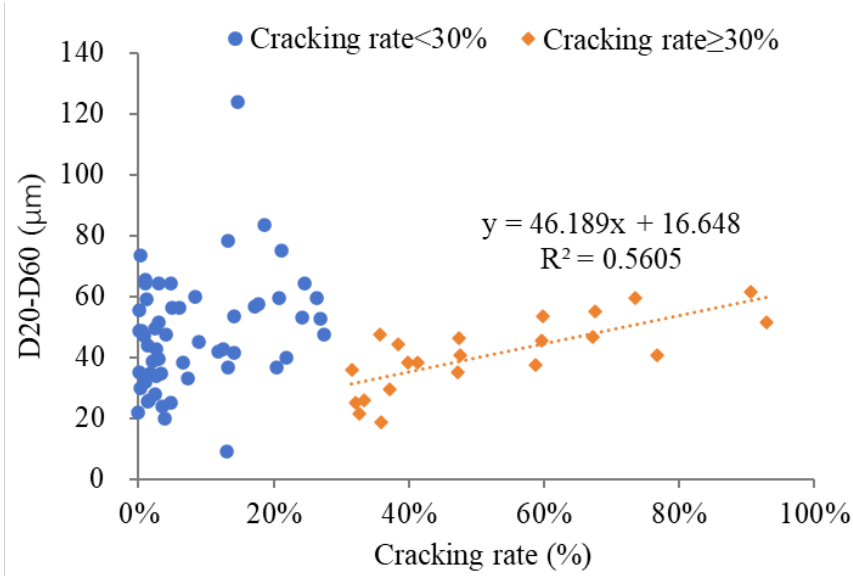


Figure 8 Correlation between  $D_{20}-D_{60}$  and cracking rate

#### 4.2.3 Field validation by on-site milling

In order to verify the evaluation results of the  $D_{20}-D_{60}$  parameter, two typical road sections were selected for on-site milling to visually inspect the actual condition of the surface layer and the base layer. Section 1 is approximately 50 meters long and is located in the middle lane. The FWD deflection test results for this section are shown in Table 3, with the red font representing the severe level. It can be observed that all  $D_{20}-D_{60}$  values for this section significantly exceed the severe threshold of 40  $\mu\text{m}$ , with some locations even surpassing 150  $\mu\text{m}$ .

Table 3 Test results of  $D_{20}-D_{60}$  for section 1

Test point	$D_{20}-D_{60}$	Test point	$D_{20}-D_{60}$	Test point	$D_{20}-D_{60}$	Test point	$D_{20}-D_{60}$
1	78.2 75.3	4	151.8 148.3	7	86.2 86.6	10	156.2 153.6
2	81.7 79.4	5	96.9 93.1	8	108.2 106.1	11	73.4 73.4
3	108.0 105.2	6	75.1 68.9	9	169.6 166.7	12	75.4 71.8

Figure 9 shows the condition of different layers in Section 1. The left part of the figure indicates that, due to recent maintenance work, the pavement surface is in good condition. However, there are alligator cracks on the surface of the lower asphalt layer, and the base layer exhibits significant raveling and non-uniformity. The right part of the figure reveals evident alligator cracks on the pavement surface. After milling, raveling is visible on the surface of the lower asphalt layer, and the base layer continues to show significant raveling. Thus, it can be concluded that the assessment based on  $D_{20}-D_{60}$  is consistent with field observations, indicating that  $D_{20}-D_{60}$  effectively reflects the structural condition of the in-service base layer.

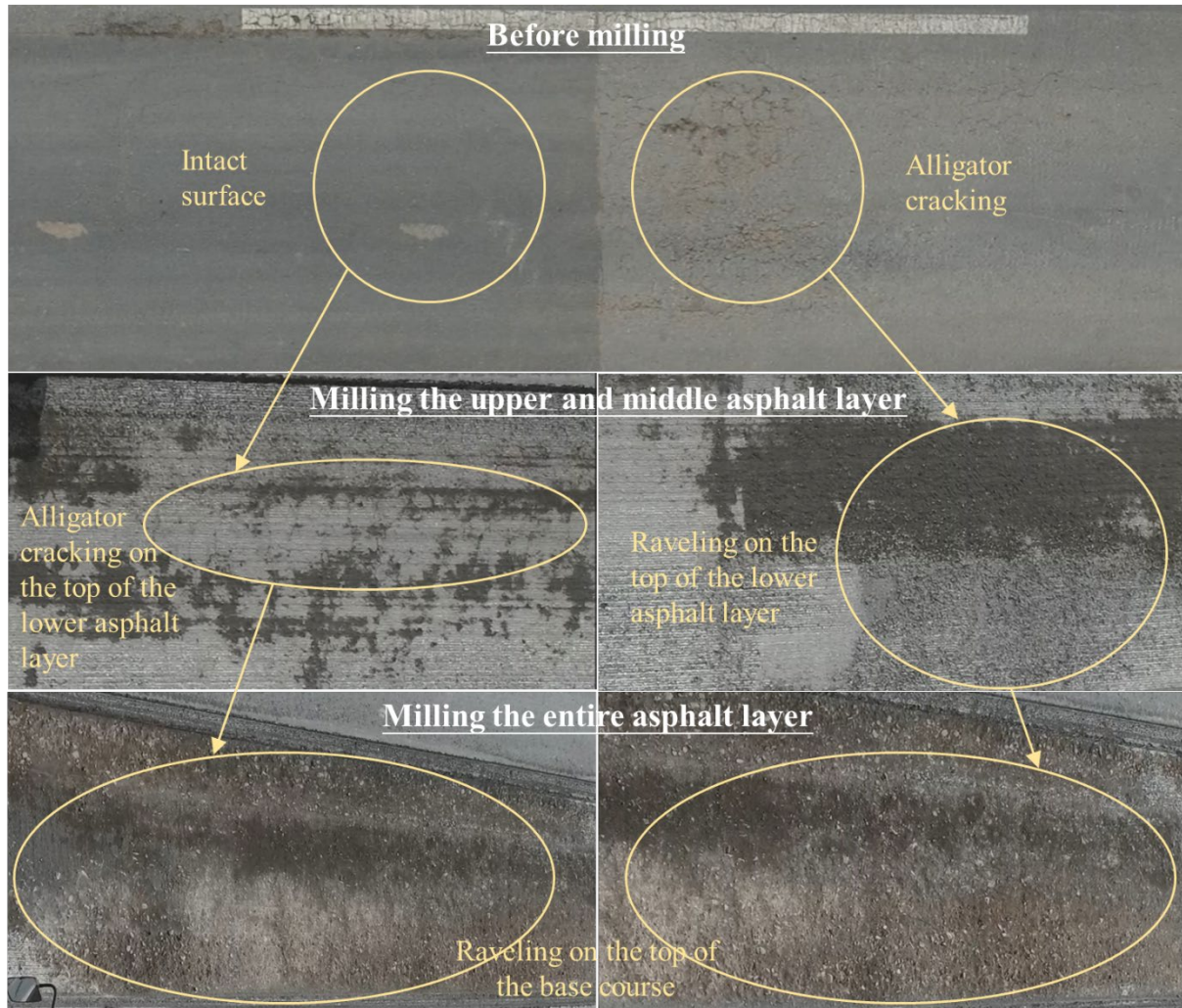


Figure 9 Structural condition of section 1

Section 2 is located in the driving lane. The FWD deflection test results for this section are presented in Table 4, with blue, orange, and red fonts representing sound, warning, and severe levels, respectively. Overall, the  $D_{20}$ - $D_{60}$  values for this section are relatively better than those for Section 1. Most of the  $D_{20}$ - $D_{60}$  values fall within the good or warning levels, with only one test point reaching the severe level.

Table 4 Test results of  $D_{20}$ - $D_{60}$  for section 2

Test point	$D_{20}$ - $D_{60}$	Test point	$D_{20}$ - $D_{60}$	Test point	$D_{20}$ - $D_{60}$	Test point	$D_{20}$ - $D_{60}$
1	24.2 24.0	4	22.2 21.1	7	33.9 34.1	10	38.4 37.9
2	17.7 18.1	5	36.9 35.6	8	87.6 86.0	11	30.0 29.9
3	12.4 12.2	6	35.7 35.3	9	39.5 39.3	12	32.3 33.2

Figure 10 shows the condition of base layers in Section 2. It can be observed that road sections with lower  $D_{20}$ - $D_{60}$  values correspondingly have good structural integrity in the base layer. In contrast, the  $D_{20}$ - $D_{60}$  value for one test point greatly exceeds the severe threshold, and the corresponding base layer shows slight raveling. This observation further validates the reliability of the  $D_{20}$ - $D_{60}$  parameter for evaluating the structural condition of the base layer.





Figure 10 Structural condition of section 2

## 5 Conclusions

Based on the FWD deflection basin data, this study identified the appropriate DBP for assessing the structural condition of semi-rigid base layers in asphalt pavements. The proposed parameter was validated through sensitivity analysis of theoretical DBP values relative to the base modulus and by examining the correlation between measured DBP values and back-calculated base modulus. Thresholds for warning and severe levels were established using  $D_{20}$ - $D_{60}$  values from sections with and without base maintenance history. Additional validation was achieved through on-site milling in a real-world R&E project, confirming the practical applicability of the findings. Based on the results of this study, the following conclusions can be drawn:

- 1)  $D_{20}$ - $D_{60}$  was the most sensitive to changes in base modulus and correlated best with the back-calculated base modulus. Therefore, it was determined to be the appropriate DBP for characterizing base structure conditions.
- 2) The thresholds for  $D_{20}$ - $D_{60}$  are 23  $\mu\text{m}$  and 40  $\mu\text{m}$ , indicating warning and severe conditions, respectively. These correspond to the potential need and the mandatory need for base maintenance.
- 3) The correlation between field  $D_{20}$ - $D_{60}$  values and pavement cracking rates suggests that a high cracking rate can indicate insufficient base strength. However, a low cracking rate does not necessarily imply an intact base structure, as pavement maintenance can restore surface conditions and mask the true condition of the base.
- 4) On-site milling further validated the above finding, demonstrating that the assessment based on  $D_{20}$ - $D_{60}$  is consistent with field observations. This indicates that  $D_{20}$ - $D_{60}$  effectively reflects the structural condition of the in-service base layer and can guide the development of treatment strategies for existing base layers in R&E projects.

While this study offers valuable contributions, some limitations remain that could be addressed in future research. One key area for further exploration is the applicability of the proposed DBP to a broader range of pavement structures and materials, such as those with thicker base layers. Validating the parameter across diverse conditions will enhance its robustness and practical relevance. To achieve this, additional field validations beyond the current case study are necessary to ensure the parameter's generalizability and consistent performance across various real-world scenarios. In addition, most FWDs are typically not equipped with a sensor at the 20cm offset, making the direct calculation of the  $D_{20}$ - $D_{60}$  parameter challenging. Although this

1 limitation could potentially be addressed using interpolation techniques and modified sensor configurations, the  
2 feasibility and effectiveness of these solutions require further assessment and validation.

### 3 **Declaration of Interest**

4 The authors declare that they have no known competing financial interests or personal relationships that could  
5 have appeared to influence the work reported in this paper.

### 6 **Acknowledgments**

7 This study was conducted under the support of Liaoning Transportation Construction Management Co.,  
8 LTD. In addition, the data used in this research were also collected from the Pavement Management System in  
9 Jiangsu province, China. The engineers and researchers who established the system and collected the data are  
10 also acknowledged for their contribution.

### **References**

- Cheng, L., Zhang, L., Lei, Y., Ma, Y., Yuan, F., Yao, P., . . . Hu, B. (2024). Evaluation of the residual fatigue life of semi-rigid base course of existing freeway using the SCB and FWD test. *International Journal of Pavement Engineering*, 25(1), 2363944
- Cui, X., Dong, Q., Ni, F., & Liang, X. (2018). Evaluation of semi-rigid base performance through numerical simulation and data mining of pavement deflection basin *Proceedings of GeoShanghai 2018 International Conference: Transportation Geotechnics and Pavement Engineering* (pp. 364-371): Springer.
- de Andrade, L. R., Bessa, I. S., Vasconcelos, K. L., Bernucci, L. L. B., & Suzuki, C. Y. (2023). Structural Performance Using Deflection Basin Parameters of Asphalt Pavements with Different Base Materials Under Heavy Traffic. *International Journal of Pavement Research and Technology*, 1-14
- Dehlen, G. (1962). A simple instrument for measuring the curvature induced in a road surfacing by a wheel load. *Civil Engineering= Siviele Ingenieurswese*, 1962(9), 189-194
- Deng, Y., & Yang, Q. (2019). Rapid evaluation of a transverse crack on a semi-rigid pavement utilising deflection basin data. *Road Materials and Pavement Design*, 20(4), 929-942
- Dong, Q., Zhao, X., Chen, X., Ma, X., & Cui, X. (2021). Long-term mechanical properties of in situ semi-rigid base materials. *Road Materials and Pavement Design*, 22(7), 1692-1707
- Donovan, P., & Tutumluer, E. (2009). Falling weight deflectometer testing to determine relative damage in asphalt pavement unbound aggregate layers. *Transportation research record*, 2104(1), 12-23
- Elshaer, M., Ghayoomi, M., & Daniel, J. S. (2020). The role of predictive models for resilient modulus of unbound materials in pavement FWD-deflection assessment. *Road Materials and Pavement Design*, 21(2), 374-392
- FHWA. (2000). Temperature Predictions and Adjustment Factors for Asphalt Pavement, Report No. FHWA-RD-98-085, 37-38
- Fuentes, L., Taborda, K., Hu, X., Horak, E., Bai, T., & Walubita, L. F. (2022). A probabilistic approach to detect structural problems in flexible pavement sections at network level assessment. *International Journal of Pavement Engineering*, 23(6), 1867-1880
- Hoffman, M. S. (1980). *Mechanistic interpretation of nondestructive pavement testing deflections*. Doctoral dissertation, University of Illinois at Urbana-Champaign.

- Horak, E., & Emery, S. (2009). Evaluation of airport pavements with FWD deflection bowl parameter benchmarking methodology *2nd European Airport Pavement Workshop, Amsterdam, The Netherlands* (pp. 13-14).
- Jiang, X., Gabrielson, J., Huang, B., Bai, Y., Polaczyk, P., Zhang, M., . . . Xiao, R. (2022). Evaluation of inverted pavement by structural condition indicators from falling weight deflectometer. *Construction and Building Materials*, 319, 125991
- Jing, C., Zhang, J., & Song, B. (2020). An innovative evaluation method for performance of in-service asphalt pavement with semi-rigid base. *Construction and Building Materials*, 235, 117376
- Kim, Y. (1998). Assessing Pavement Layer Condition Using Deflection Data. National Cooperative Highway Research Program Project 10-48. *Transportation Research Board, Washington DC*
- Kutay, M. E., Chatti, K., & Lei, L. (2011). Backcalculation of dynamic modulus mastercurve from falling weight deflectometer surface deflections. *Transportation research record*, 2227(1), 87-96
- Li, J., Liao, C., Xiong, C., Chen, C., Wang, Z., Wu, C., . . . Xu, X. (2023). Research on distresses detection, evaluation and maintenance decision-making for highway pavement in reconstruction and expansion project. *Case Studies in Construction Materials*, 19, e02451
- Liang, H., Gong, H., Sun, Y., Shi, J., Cong, L., Han, W., & Guo, P. (2023). Investigating long-term performance of flexible pavement using Bayesian multilevel models. *Road Materials and Pavement Design*, 24(8), 1995-2009
- Liu, Z., Yang, Q., & Gu, X. (2023). Assessment of pavement structural conditions and remaining life combining accelerated pavement testing and ground-penetrating radar. *Remote Sensing*, 15(18), 4620
- Ma, L., Li, M., Pang, J., & Huang, C. (2019). Evaluation of transverse cracks for semi-rigid asphalt pavements using deflection basin parameters. *Transportation Research Record*, 2673(2), 358-367
- Ministry of Transport of the People's Republic of China. (2017). Specifications for Design of Highway Asphalt Pavement (JTG D50-2017).
- Ministry of Transport of the People's Republic of China. (2018). Highway Performance Assessment Standards (JTG H20-2018).
- Ministry of Transport of the People's Republic of China. (2019). Field Test Methods of Highway Subgrade and Pavement (JTG 3450—2019).
- Nguyen, T., Tan, J. Y., & Ho, N. Y. (2023). Deflection bowl parameters for falling weight deflectometer testing: data collection and threshold benchmarking. *International Journal of Pavement Engineering*, 24(2), 2034815
- Park, H. M., Kim, Y. R., & Wan Park, S. (2005). Assessment of pavement layer condition with use of multiload-level falling weight deflectometer deflections. *Transportation research record*, 1905(1), 107-116
- Pierce, L. M., Bruinsma, J. E., Smith, K. D., Wade, M. J., Chatti, K., & Vandenbossche, J. (2017). *Using falling weight deflectometer data with mechanistic-empirical design and analysis, volume III: Guidelines for deflection testing, analysis, and interpretation*.
- Pożarycki, A., Górnaś, P., & Wanatowski, D. (2019). The influence of frequency normalisation of FWD pavement measurements on backcalculated values of stiffness moduli. *Road Materials and Pavement Design*, 20(1), 1-19
- Rabbi, M. F., & Mishra, D. (2021). Using FWD deflection basin parameters for network-level assessment of flexible pavements. *International Journal of Pavement Engineering*, 22(2), 147-161



- Talvik, O., & Aavik, A. (2009). Use of FWD deflection basin parameters (SCI, BDI, BCI) for pavement condition assessment. *The Baltic Journal of road and bridge engineering*, 4(4), 196-202
- Vaitkus, A., Gražulytė, J., Kravcovas, I., & Mickevič, R. (2021). Comparison of the bearing capacity of pavement structures with unbound and cold central-plant recycled base courses based on FWD data. *Sustainability*, 13(11), 6310
- Vyas, V., Singh, A. P., & Srivastava, A. (2021). Prediction of asphalt pavement condition using FWD deflection basin parameters and artificial neural networks. *Road Materials and Pavement Design*, 22(12), 2748-2766
- Xiong, C., Yu, J., & Zhang, X. (2023). Use of NDT systems to investigate pavement reconstruction needs and improve maintenance treatment decision-making. *International Journal of Pavement Engineering*, 24(1), 2011872
- Xu, B., Ranjithan, S. R., & Kim, Y. R. (2002). New relationships between falling weight deflectometer deflections and asphalt pavement layer condition indicators. *Transportation research record*, 1806(1), 48-56
- Xu, Y., Shi, X., & Yao, Y. (2024). Performance Assessment of Existing Asphalt Pavement in China's Highway Reconstruction and Expansion Project Based on Coupling Weighting Method and Cloud Model Theory. *Applied Sciences* (2076-3417), 14(13)
- Yao, L., Leng, Z., Jiang, J., & Ni, F. (2022). Modelling of pavement performance evolution considering uncertainty and interpretability: a machine learning based framework. *International Journal of Pavement Engineering*, 23(14), 5211-5226
- Ye, X., Chen, Y., & Chen, C. (2019). Study on traffic organization and work-zone optimization of four-lane freeway reconstruction and expansion *Journal of Physics: Conference Series* (Vol. 1187, pp. 052102): IOP Publishing.
- Zang, G., Sun, L., Chen, Z., & Li, L. (2018). A nondestructive evaluation method for semi-rigid base cracking condition of asphalt pavement. *Construction and Building Materials*, 162, 892-897
- Zhang, Z., Claros, G., Manuel, L., & Damjanovic, I. (2003). Evaluation of the pavement structural condition at network level using falling weight deflectometer (FWD) data *82nd Transportation Research Board meeting, Washington, DC, USA*